Electronic Supplementary Information

POSS and imidazolium-constructed ionic porous hypercrosslinked polymers with multiple active sites for synergistic catalytic CO_2 transformation

Yadong Zhang[#], Ke Liu[#], Lei Wu[#], He Huang, Zixuan Xu, Zhouyang Long, Minman Tong, Yingqiu Gu*, Zhenglong Qin* and Guojian Chen*

School of Chemistry and Materials Science, Jiangsu Key Laboratory of Green Synthetic Chemistry for Functional Materials, Jiangsu Normal University, No. 101, Shanghai Road, Tongshan District, Xuzhou 221116, Jiangsu, China.

* Corresponding authors, E-mail addresses:

guyingqiu@jsnu.edu.cn (Y. Gu); hxxqzl@jsnu.edu.cn (Z. Qin); gjchen@jsnu.edu.cn (G. Chen).

[#] These authors contributed equally to this work.

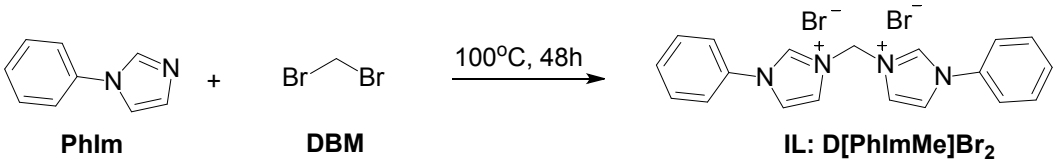

Scheme S1 Synthesis of imidazolium ionic liquid (IL) crosslinker D[PhImMe]Br_2.

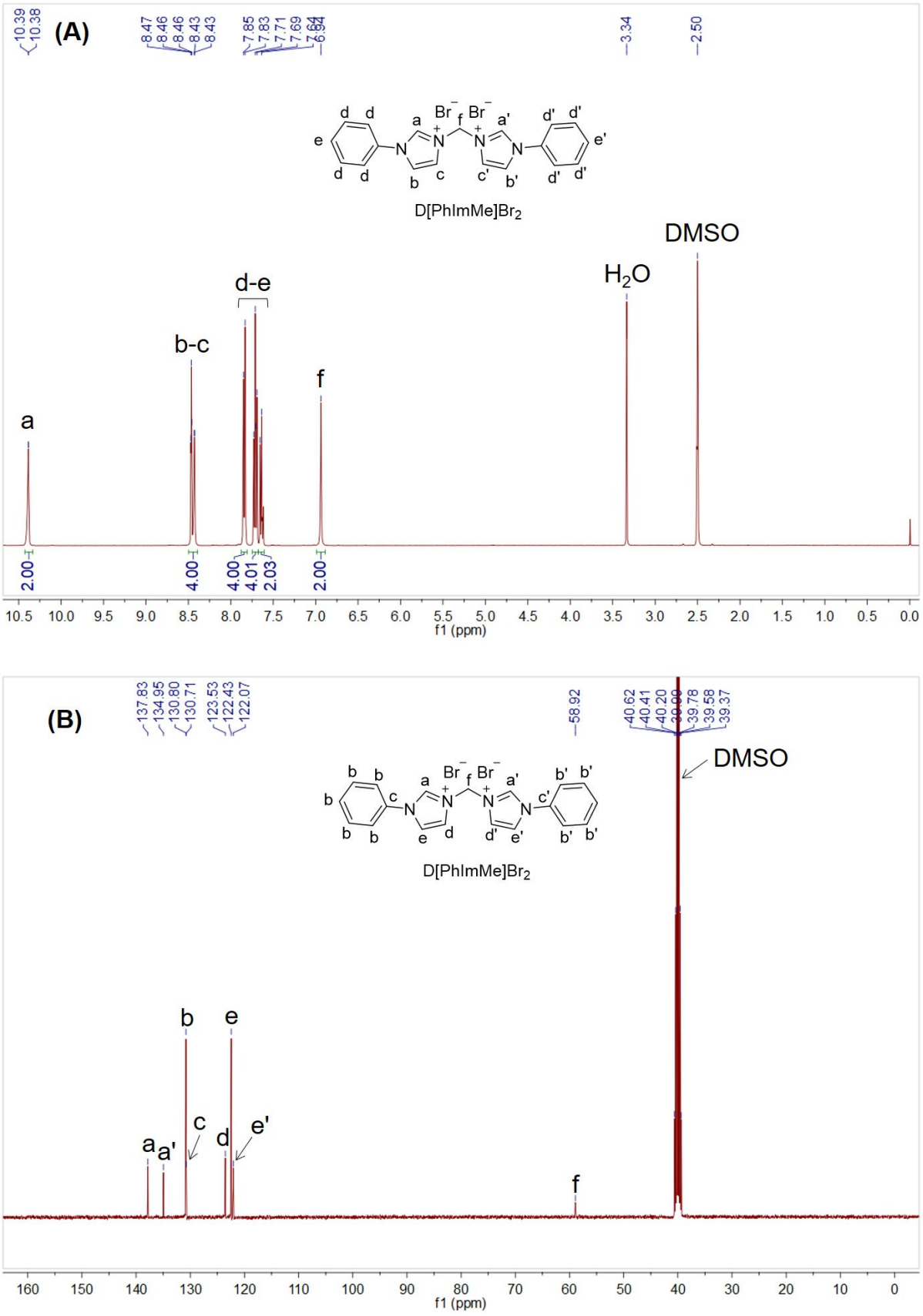

Fig. S1 (A) ^{1}H NMR and (B) ^{13}C NMR spectra of D[PhImMe]Br_2 in the solvent d_6-DMSO.

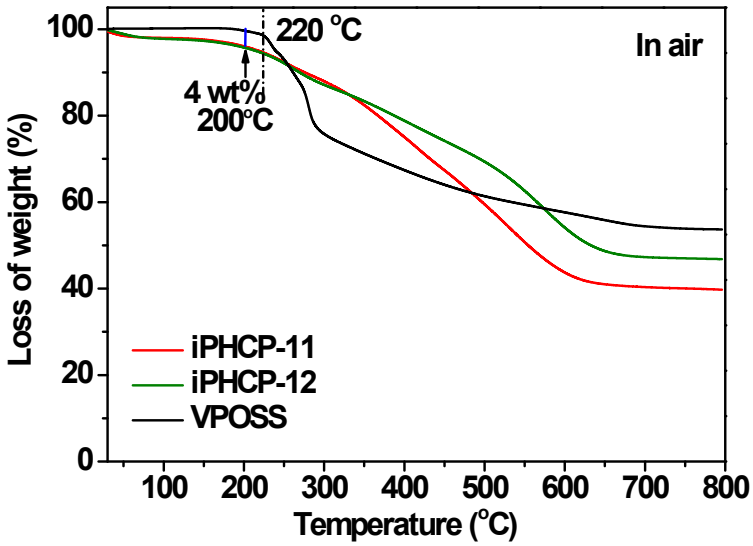

Fig. S2 Thermogravimetric analysis (TGA) curves of VPOSS, iPHCP-11 and iPHCP-12 under air atmosphere.

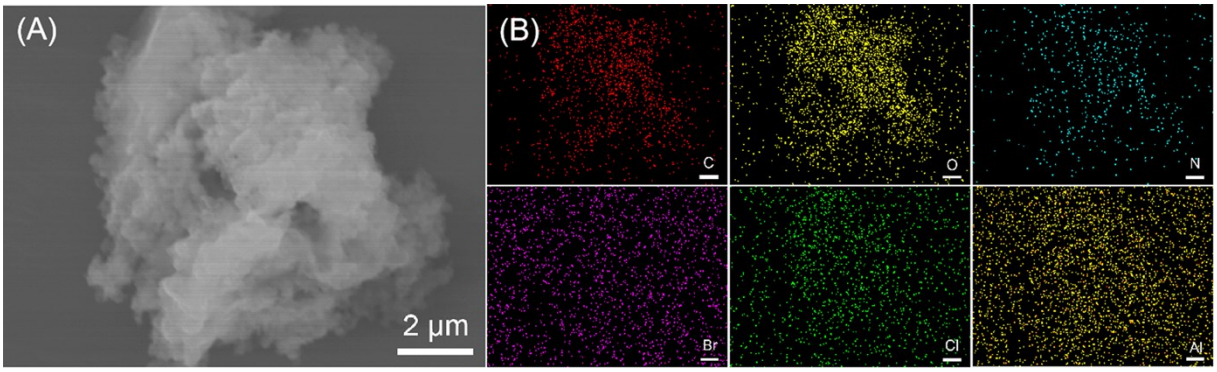

Fig. S3 (A) SEM and (B) Energy-dispersive X-ray spectrometry (EDS) elemental mapping images including C, O, N, Br, Cl and Al elements for the sample iPHCP-12.

Table S1 The detailed comparisons of the catalytic activity of iPHCP-12 with other metal-based POP and iPOP heterogeneous catalysts in the synthesis of cyclic carbonate from epichlorohydrin and CO_2.[a]

Entry	Catalyst	Cocatalyst [b]	The amount of substrate /catalyst [c]	*P* (MPa)	*T* (^oC)	*t* (h)	Yield (%)	Ref.
1	Zn-CMP	TBAB	50 mmol/0.2 mol% [Zn]	3	120	1	99.6	S1
2	Cr-CMP	TBAB	25 mmol/0.1 g	3	100	2	99.1	S2
3	Bp-Zn@MA	TBAB	6.72 mmol/0.02 g	1	100	1.5	97	S3
4	Cu/POP-Bpy	TBAB	10 mmol/0.5 mol % [Cu]	0.1	29	48	99	S4
5	Co/POP-TPP	TBAB	12.5 mmol/0.05 g	0.1	29	24	95.6	S5
6	HUST-1-Co	TBAB	25 mmol/0.02 g	0.1	25	48	94.7	S6
7	Py-Zn@MA	none	6.11 mmol/0.02 g	2	130	6	96	S7
8	TBB-Bpy@Salen-Co	none	20 mmol/0.05 g	1	80	6	95	S8
9	Co-Salen-TBB-Py	none	20 mmol/0.05 g	0.5	80	8	93.8	S9
10	DVB@ISA	none	6 mmol/0.25 mol%	1	60	24	98	S10
11	Al-iPOP-1	none	3 mmol/0.1 mol%	1	40	6	98	S11
12	SYSU-Zn@IL2	none	3 mmol/0.16 mol%	1	80	12	99	S12
13	Al-CPOP	none	10 mmol/1 mol%	0.1	120	24	95	S13
14	ZnTPy-BIM4/CNTs-3	none	13.27 mmol/0.069 mol%	1.5	120	2.5	98	S14
15	POF-Zn^{2+}-I^-	none	50 mmol/0.3%	1	60	8	92.2	S15
16	NHC-CAP-1(Zn^{2+})	none	41.5 mmol/0.025 g	2	100	3	97	S16
17	PPh_3-ILBr-$ZnBr_2$@POPs	none	56 mmol/0.0163 g	3	120	1	37	S17
18	Zn-CIF2-C_2H_4	none	3 mmol/0.18 mol%	2.5	120	4	98	S18
19	$ZnBr_2$@Bpy-PHP-4	none	2 mmol/0.05 g	0.1	80	72	99	S19
20	iPHCP-12	none	2 mmol/0.05 g	0.1	60	60	99	Present

[a] It should be pointed out that different catalysts were evaluated under different conditions (reaction temperature, CO_2 pressure, the amount of substrate/catalyst, solvent, *etc*.), thus it is difficult to directly compare the activity between different catalytic systems. The represented catalytic activities using yields of the product in Table S1 were obtained under their own optimized conditions, which should be considered in a reasonable comparison; [b] The cocatalyst is tetra-*n*-butyl-ammonium bromide (TBAB). [c] The data for the amount of substrate/catalyst was collected from the original literatures, the amount of catalyst was shown using mol% based on substrate (mmol) or the mass of catalysts.

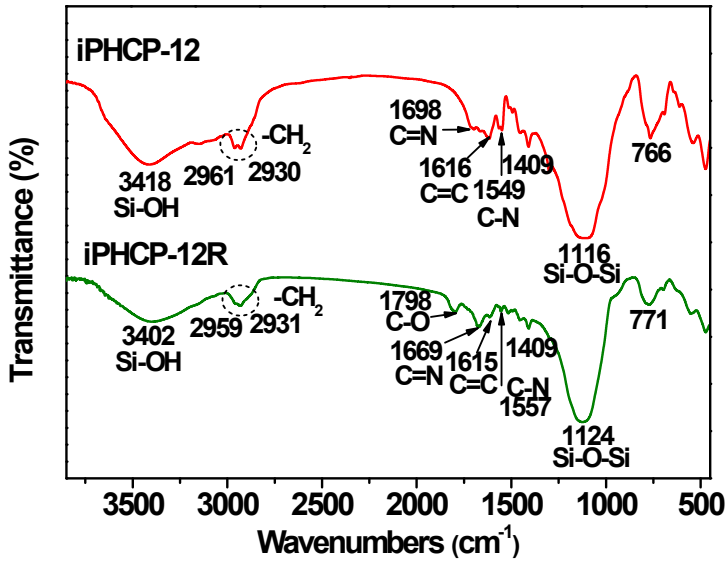

Fig. S4 FTIR spectra of the fresh catalyst iPHCP-12 and the reused catalyst iPHCP-12R after five runs.

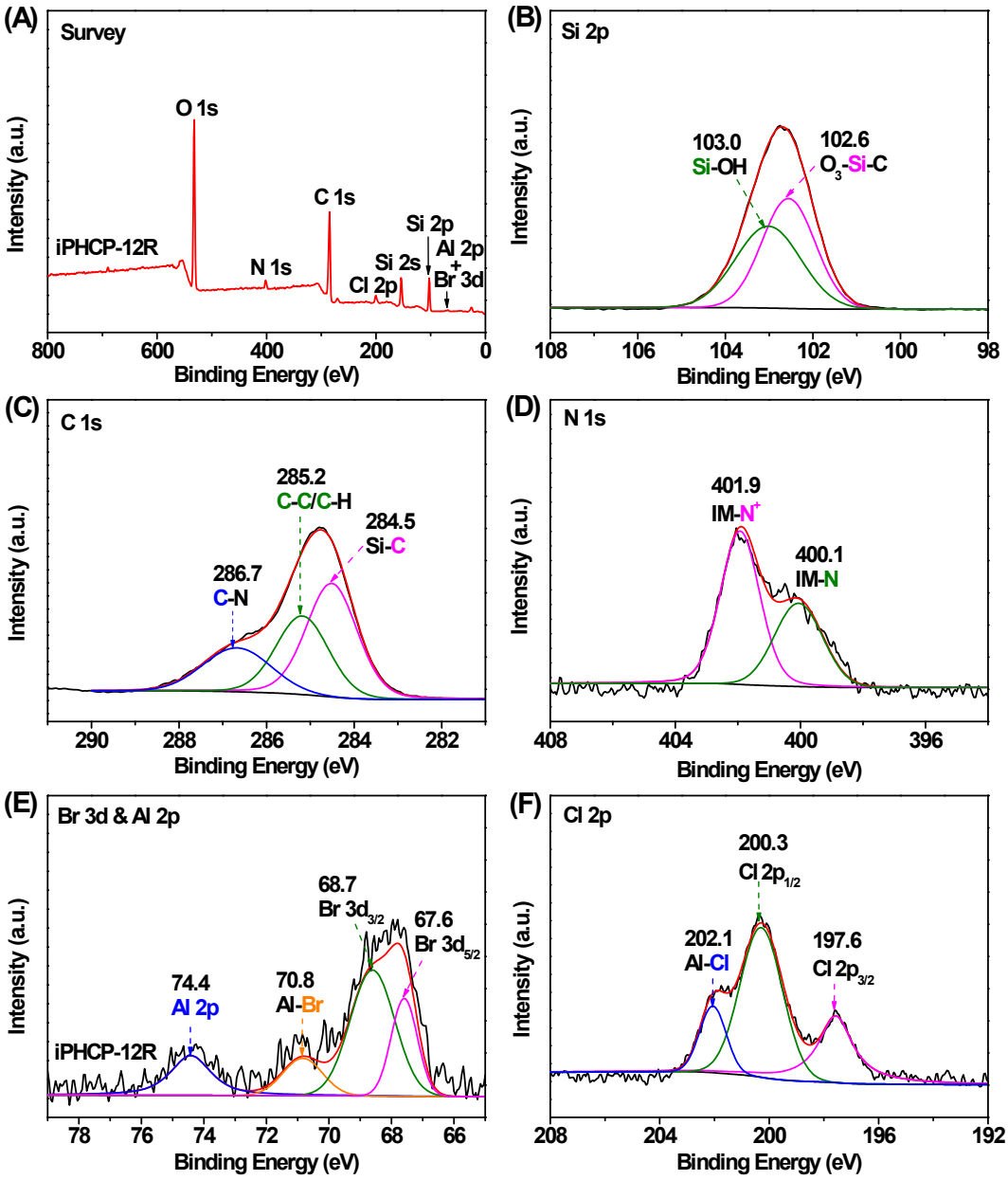

Fig. S5 (A) XPS spectrum survey, (B) Si 2p, (C) C 1s, (D) N 1s, (E) Br 3d & Al 2p and (F) Cl 2p for the reused catalyst iPHCP-12R.

Table S2 The elemental compositions of the fresh catalyst iPHCP-12 and reused iPHCP-12R detected from XPS. [a]

Sample	C (at%)	Si (at%)	O (at%)	N (at%)	Br (at%)	Cl (at%)	Al (at%)
The fresh iPHCP-12	48.40	15.67	27.56	3.85	1.37	2.54	0.62
The reused iPHCP-12R	46.86	15.53	32.00	3.21	1.12	2.08	0.51

[a] All elemental compositions were presented by the atomic concentration (at%).

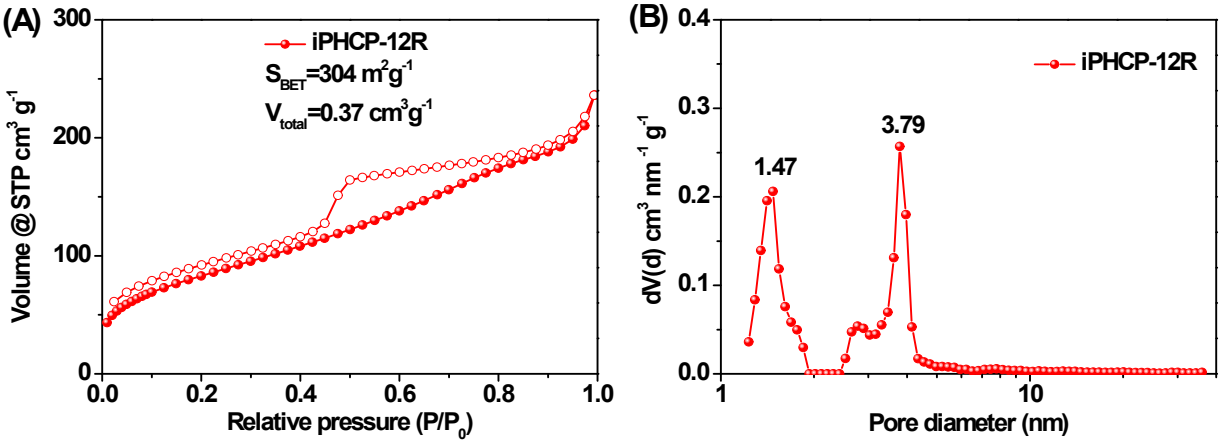

Fig. S6 (A) N_2 sorption isotherms and (B) NLDFT pore size distribution of the reused catalyst iPHCP-12R.

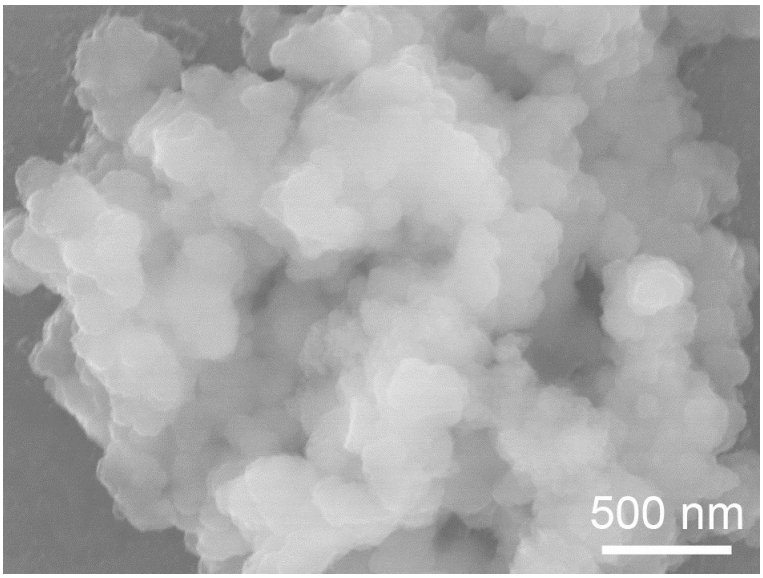

Fig. S7 The SEM image of the reused catalyst iPHCP-12R.

Characterizations for the reused catalyst iPHCP-12R

FTIR and XPS were used to characterize chemical structure and elemental composition of the reused catalyst iPHCP-12R, as shown in Fig. S4, Fig. S5 and Table S2. The characteristic peaks of reused iPHCP-12R in the FTIR spectrum were almost identical to the fresh catalyst (Fig. S4). However, one new absorption peak was observed at 1798 cm^{-1}, attributing to the C=O stretching band of the cyclic carbonate that was slightly adsorbed within the catalyst. Compared with the fresh catalyst iPHCP-12, the XPS spectra and elemental compositions and chemical states for Si, C, N, Br, Al and Cl in the reused iPHCP-12R only have slight changes (Fig. S5 and Table S2), indicating its relatively well-preserved chemical compositions. Additionally, iPHCP-12R was characterized by N_2 sorption experiment (Fig. S6) and the SEM image (Fig. S7). The S_{BET} and V_{total} values of iPHCP-12R slightly decrease compared with the fresh one, due to the adsorbed product within the pore of the catalyst. As described in the SEM image, the porous structure and morphology of iPHCP-12R was well retained.

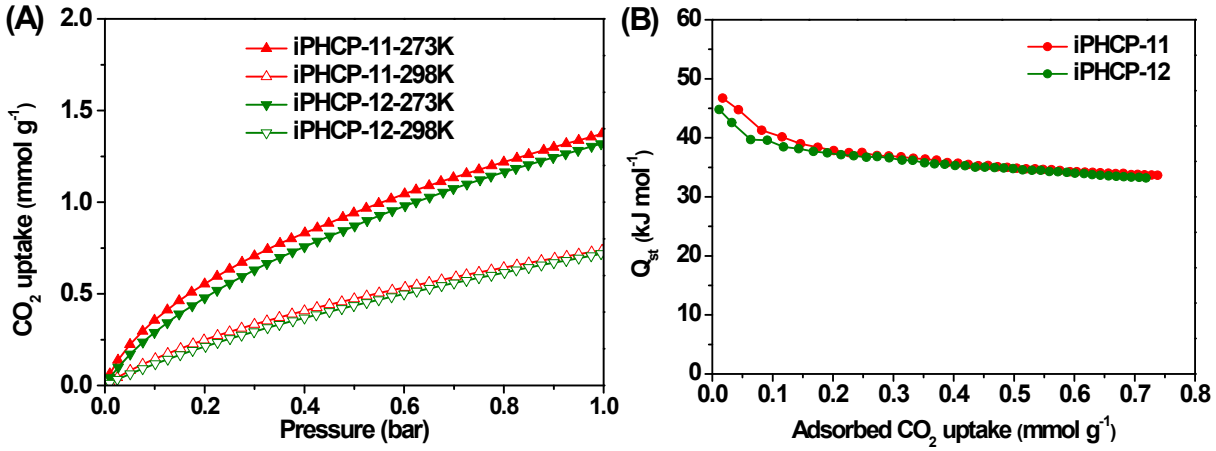

Fig. S8 (A) CO_2 adsorption isotherms of iPHCP-11 and iPHCP-12 collected up to 1.0 bar at 273 K and 298 K. (B) The isosteric heat (Q_{st}) plots of CO_2 adsorption for iPHCP-11 and iPHCP-12 calculated using the Clausius-Clapeyron equation.

[1]H NMR spectra and data for the crude cyclic carbonates (Fig. S9-S18)

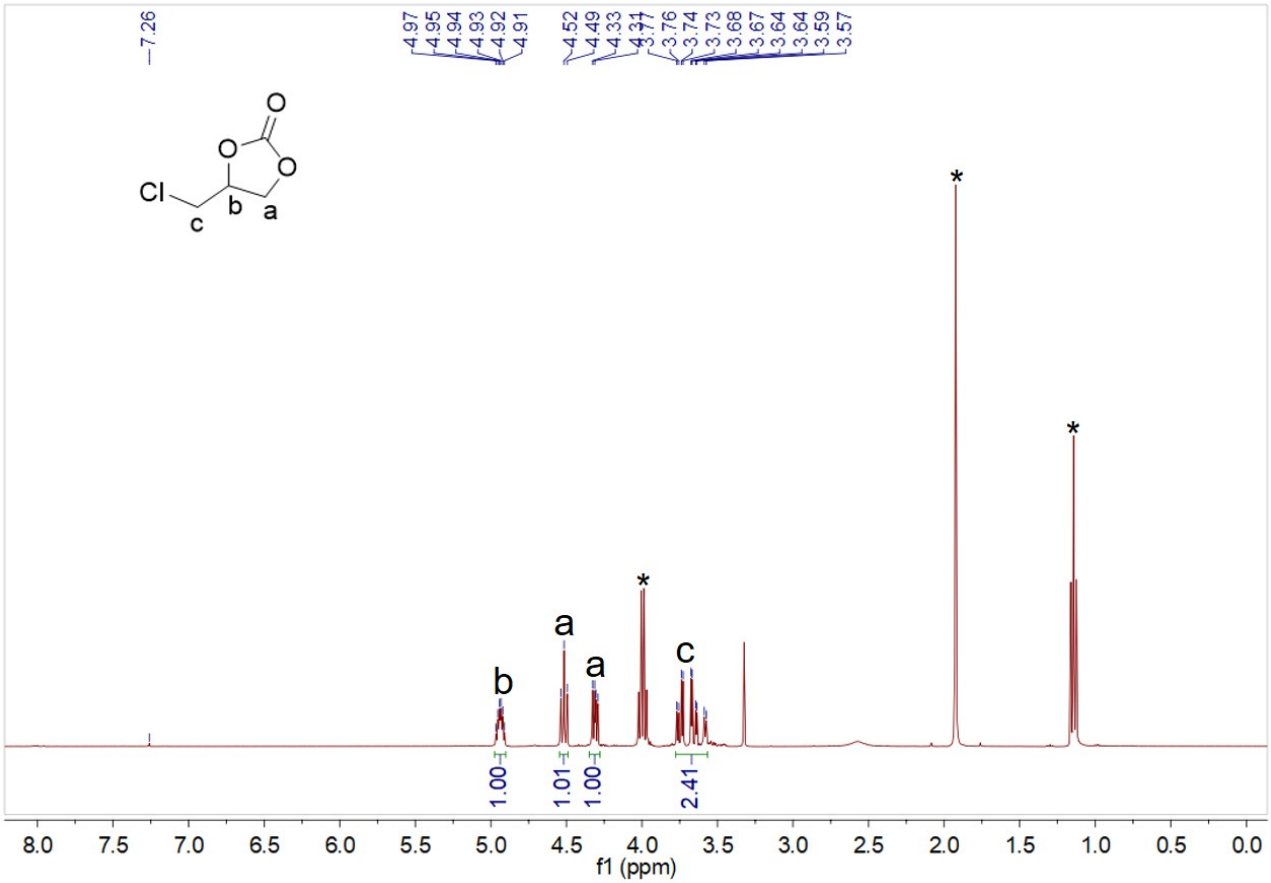

Fig. S9 [1]H NMR spectrum of 4-(chloromethyl)-1,3-dioxolan-2-one (400 MHz, $CDCl_3$): δ 4.94 (1H, CH), 4.52 (1H, CH_2), 4.31 (1H, CH_2), 3.78~3.57 ppm (2H, CH_2). * represents the residual solvent ethyl acetate.

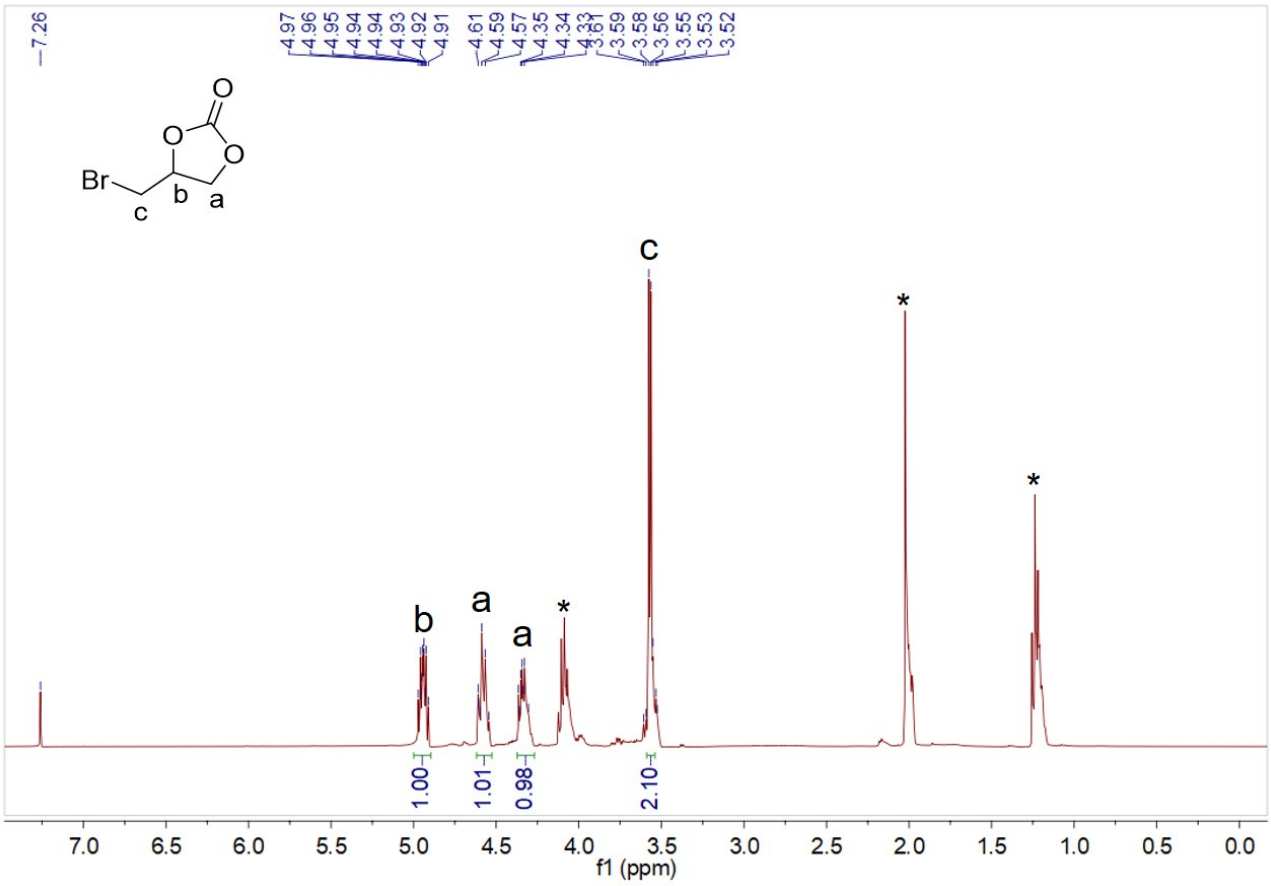

Fig. S10 ^{1}H NMR spectrum of 4-(bromomethyl)-1,3-dioxolan-2-one (400 MHz, $CDCl_3$): δ 4.94 (1H, CH), 4.59 (1H, CH_2), 4.34 (1H, CH_2), 3.56 ppm (2H, CH_2). * represents the residual solvent ethyl acetate.

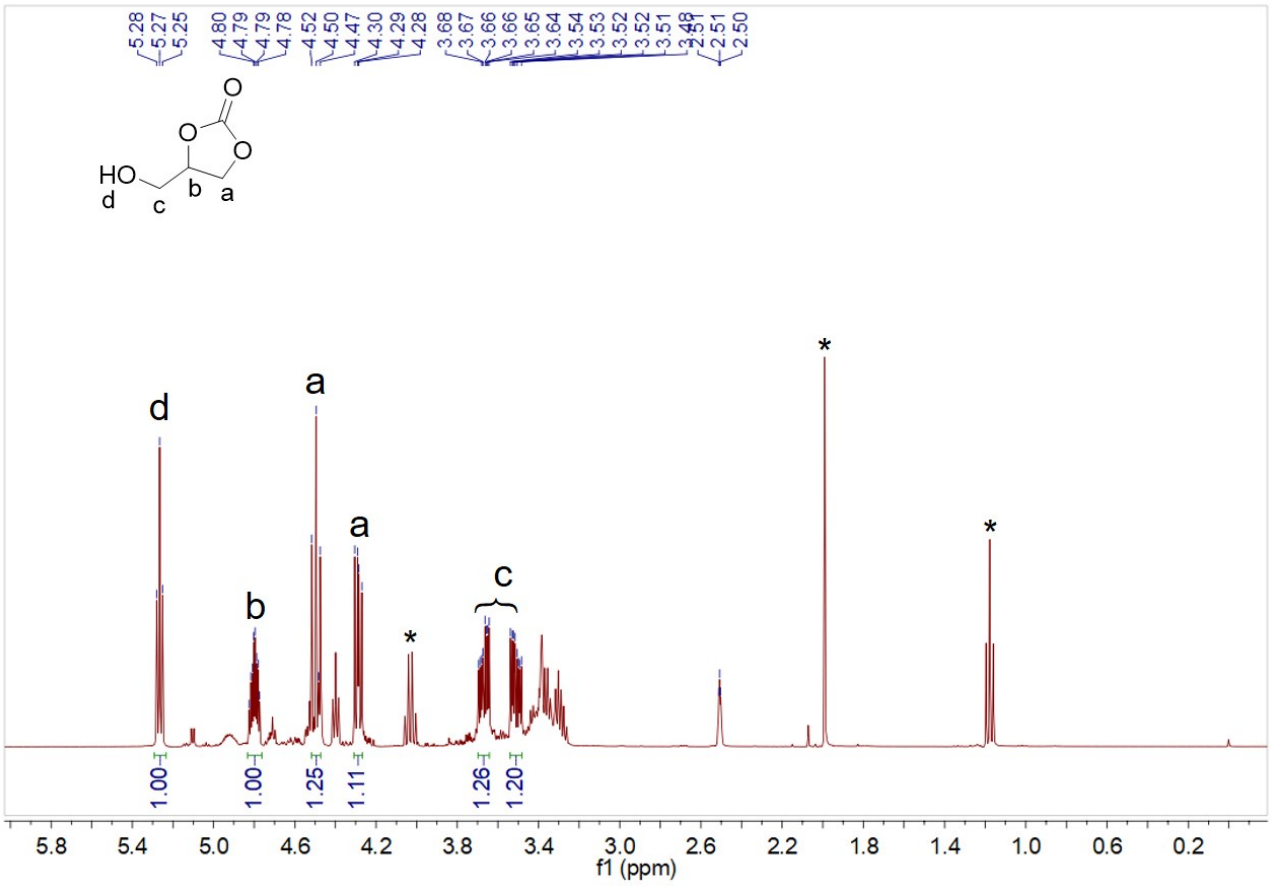

Fig. S11 ^{1}H NMR spectrum of 4-(hydroxymethyl)-1,3-dioxolan-2-one (400 MHz, DMSO): δ 5.27 (1H, OH), 4.80 (1H, OCH), 4.49 (1H, CH_2O), 4.29 (1H, CH_2O), 3.67 (1H, CH_2OH), 3.51 ppm (1H, CH_2OH). * represents the residual solvent ethyl acetate.

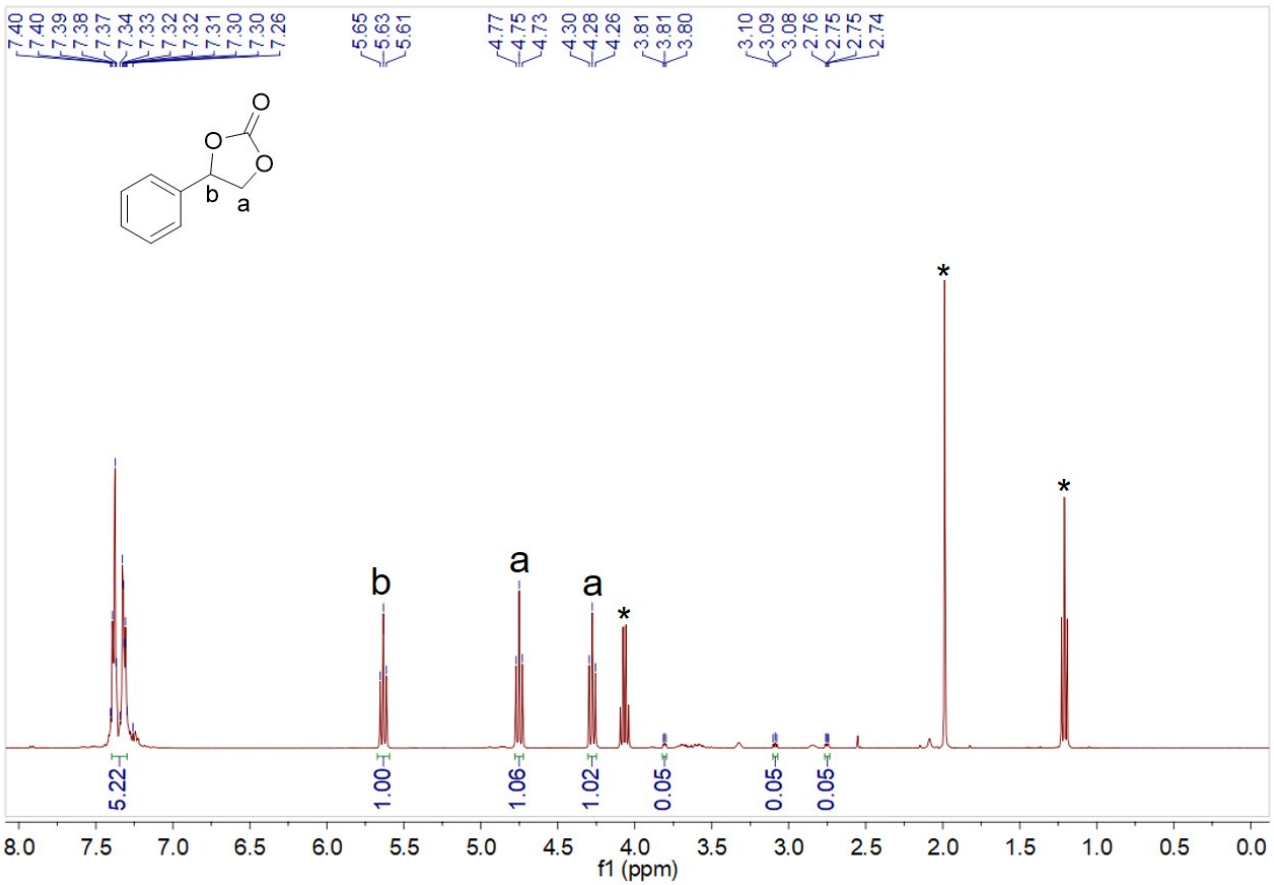

Fig. S12 ^{1}H NMR spectrum of 4-phenyl-1,3-dioxolan-2-one (400 MHz, $CDCl_3$): δ 7.40~7.30 (5H, CH), 5.63 (1H, CH_2), 4.75 (1H, CH_2), 4.28 ppm (1H, CH_2). * represents the residual solvent ethyl acetate.

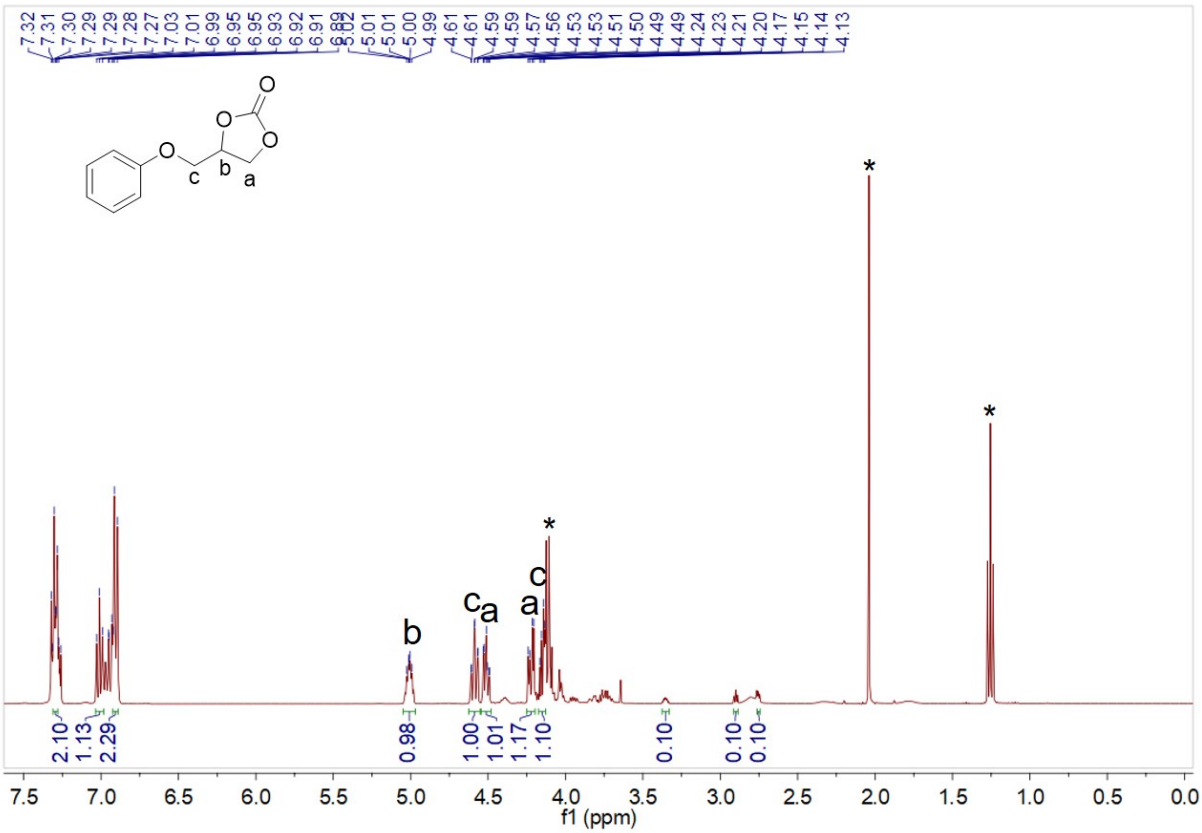

Fig. S13 ^{1}H NMR spectrum of 4-(phenoxymethyl)-1,3-dioxolan-2-one (400 MHz, $CDCl_3$): δ 7.29 (2H, CH), 7.01 (1H, CH), 6.91 (2H, CH), 5.05~4.97 (1H, CH), 4.59 (1H, CH_2), 4.54~4.48 (1H, CH_2), 4.22 (1H, CH_2), 4.15 ppm (1H, CH_2). * represents the residual solvent ethyl acetate.

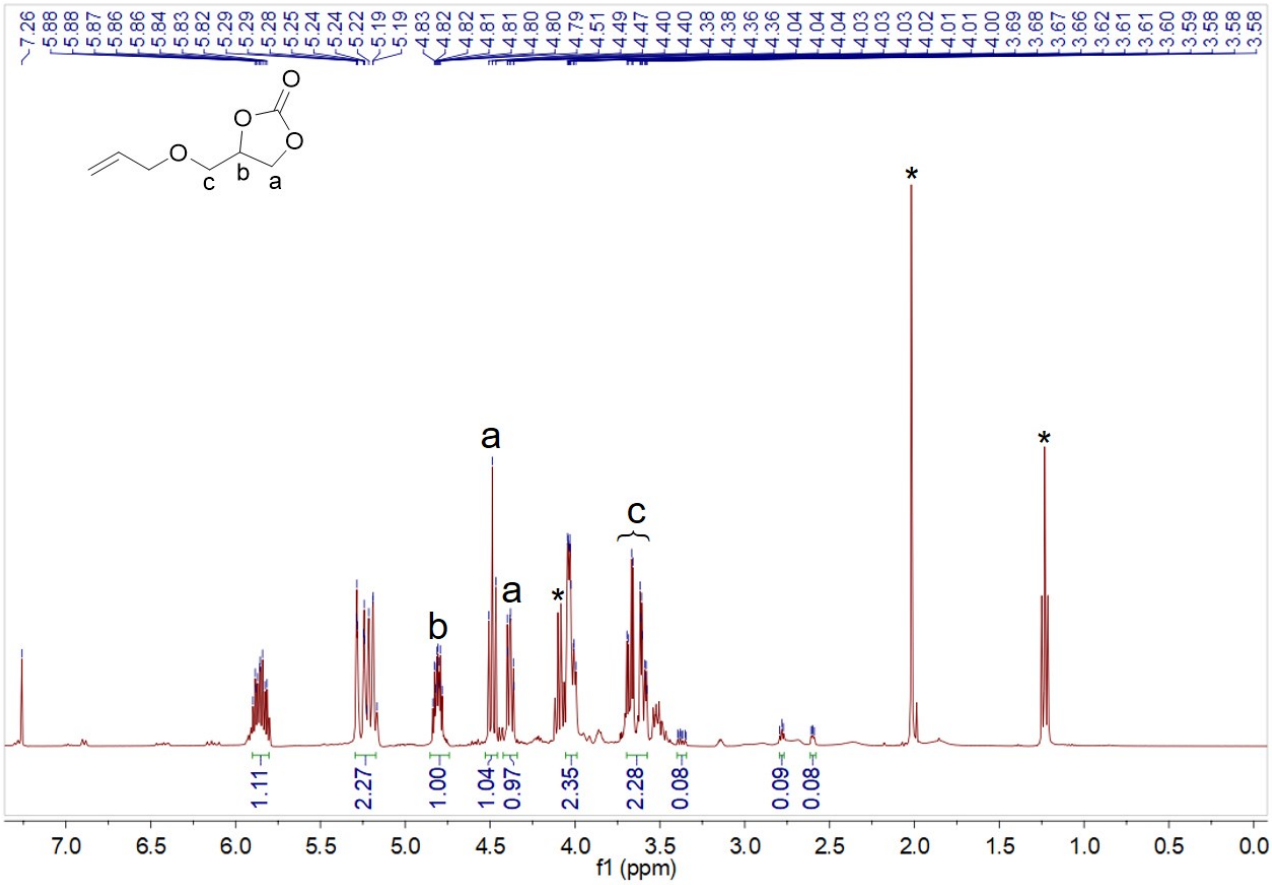

Fig. S14 ^{1}H NMR spectrum of allyloxymethyl-1,3-dioxolan-2-one (400 MHz, $CDCl_3$): δ 5.90~5.80 (1H, CH), 5.30~5.17 (2H, CH_2), 4.81 (1H, CH), 4.49 (1H, CH_2), 4.42~4.34 (1H, CH_2), 4.06~3.99 (2H, CH_2), 3.70~3.58 ppm (2H, CH_2). * represents the residual solvent ethyl acetate.

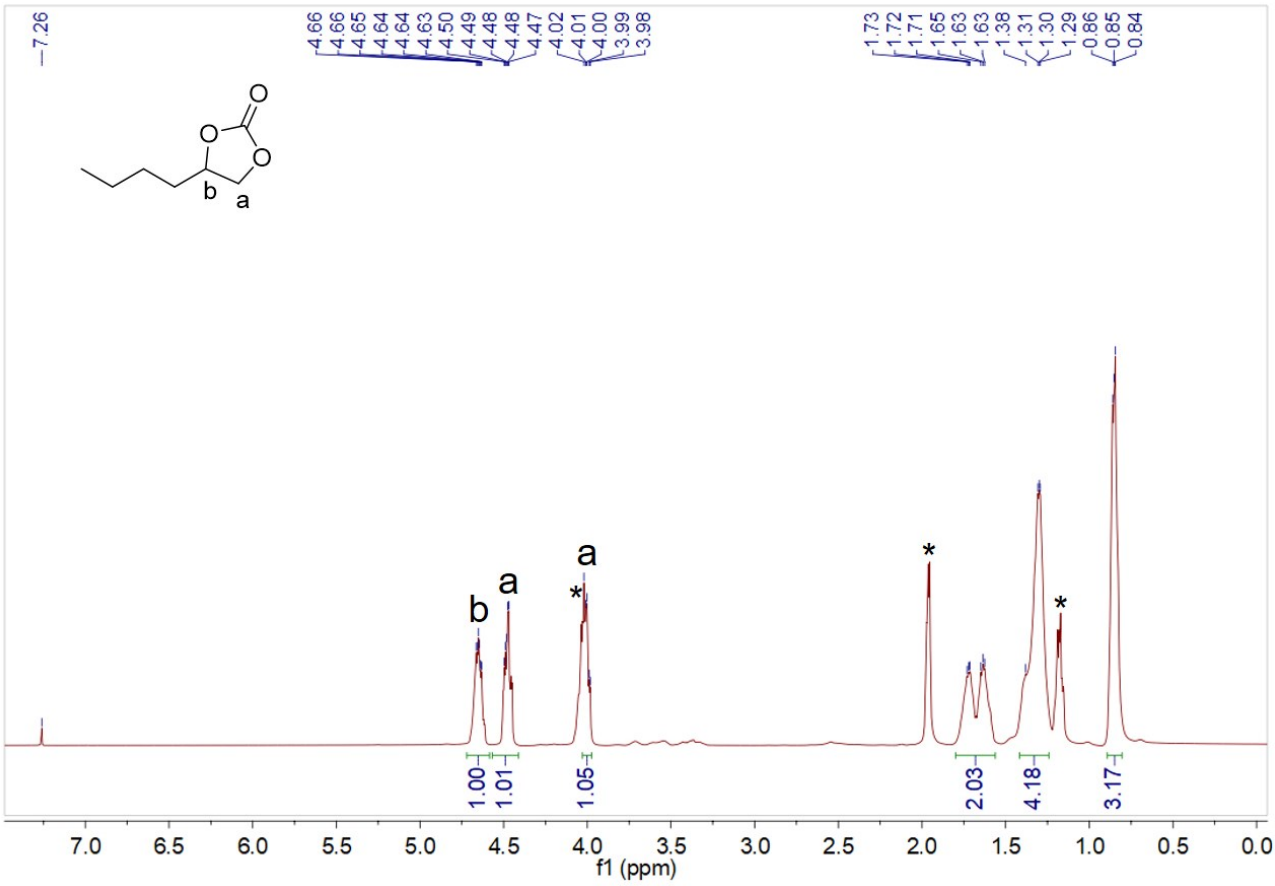

Fig. S15 ^{1}H NMR spectrum of 4-butyl-1,3-dioxolan-2-one (400 MHz, $CDCl_3$): δ 4.72~4.58 (1H, CH_2), 4.57~4.41 (1H, CH_2), 4.03~3.97 (1H, CH_2), 1.80~1.56 (2H, CH_2), 1.32 (4H, CH_2), 0.89~0.80 (3H, CH_3). * represents the residual solvent ethyl acetate.

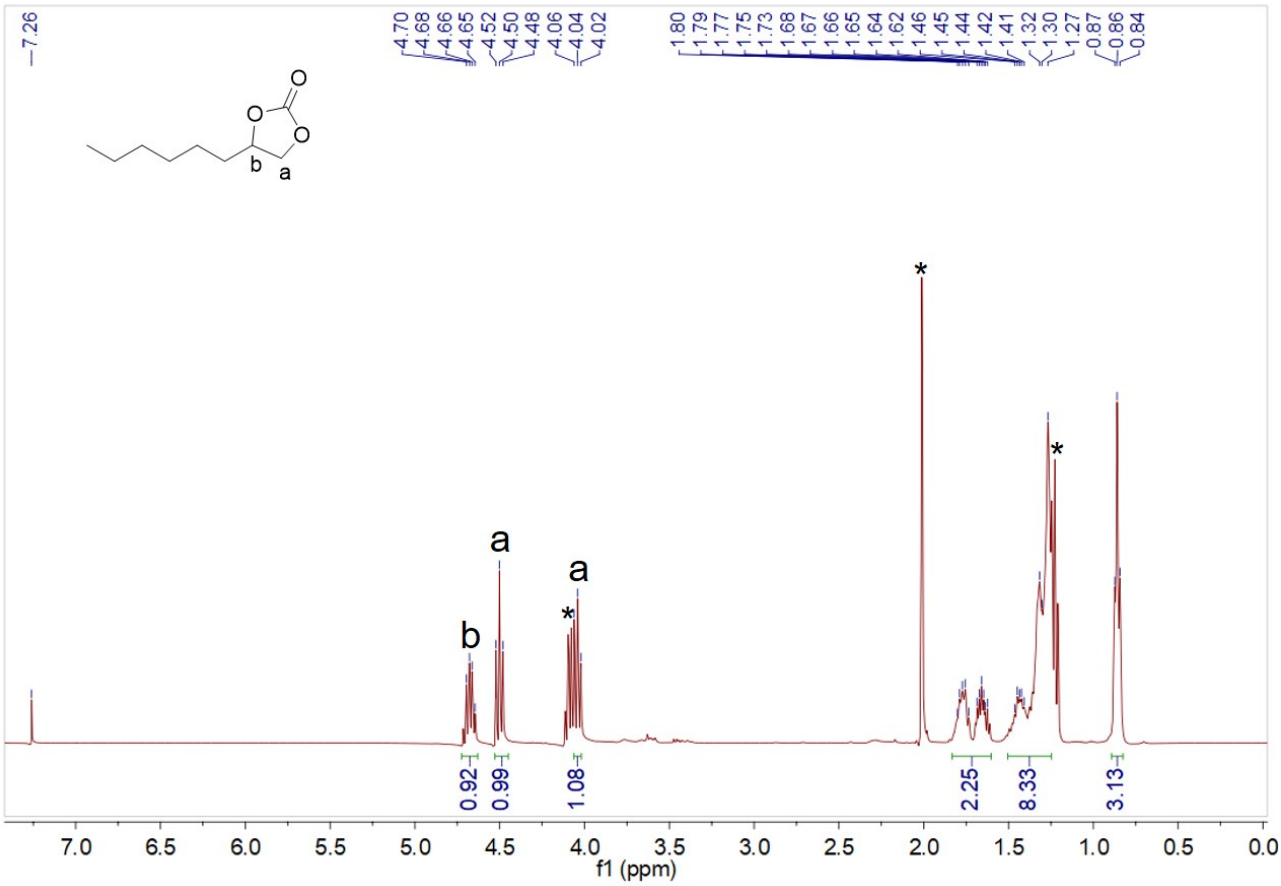

Fig. S16 ^{1}H NMR spectrum of 4-hexyl-1,3-dioxolan-2-one (400 MHz, $CDCl_3$): δ 4.67 (1H, CH_2), 4.50 (1H, CH_2), 4.06~4.02 (1H, CH_2), 1.83~1.60 (2H, CH_2), 1.51~1.25 (8H, CH_2), 0.86 ppm (3H, CH_3). * represents the residual solvent ethyl acetate.

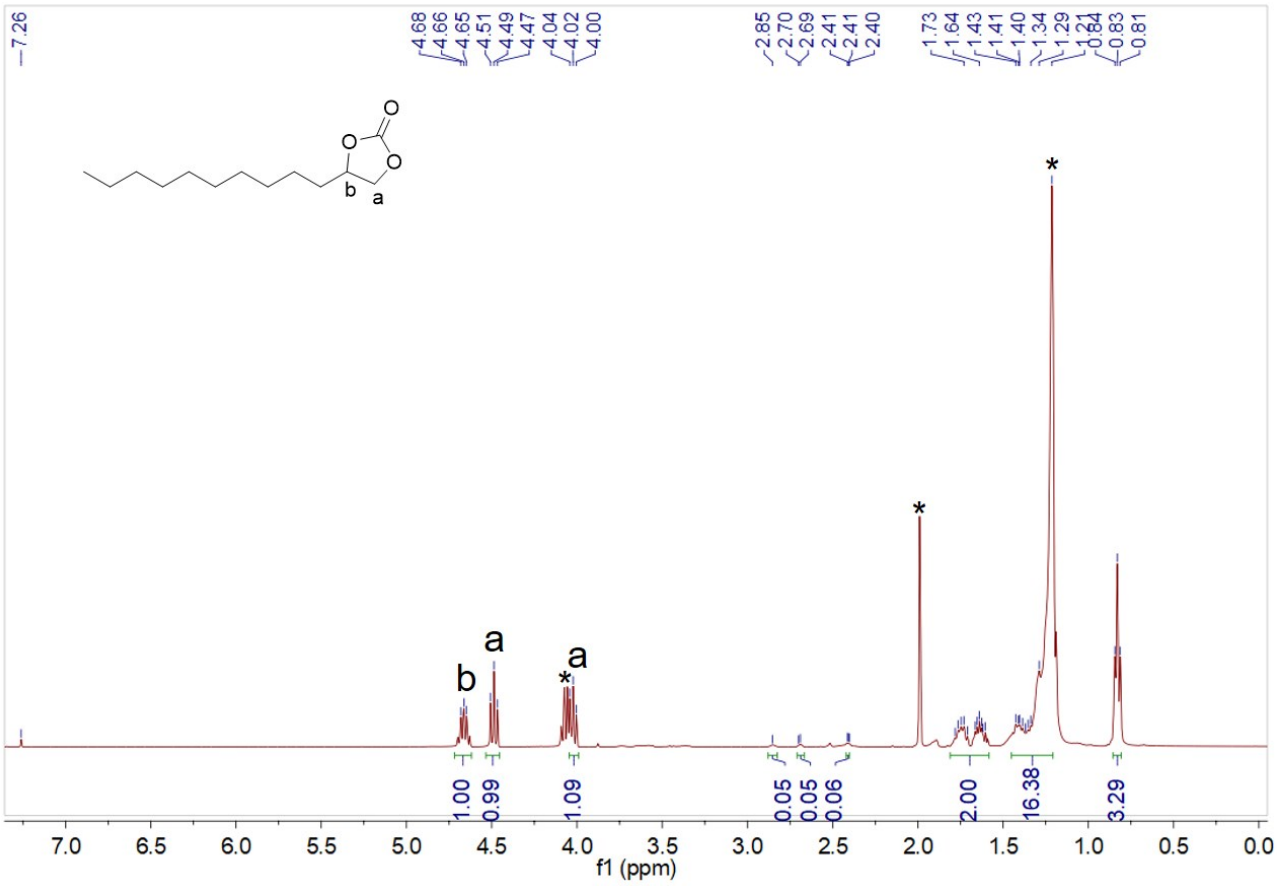

Fig. S17 ^{1}H NMR spectrum of 4-decyl-1,3-dioxolan-2-one (400 MHz, $CDCl_3$): δ 4.72~4.62 (1H ,CH_2), 4.49 (1H, CH_2), 4.02 (1H, CH_2), 1.81~1.58 (2H, CH_2), 1.45~1.21 (16H, CH_2), 0.86 ppm (3H, CH_3). * represents the residual solvent ethyl acetate.

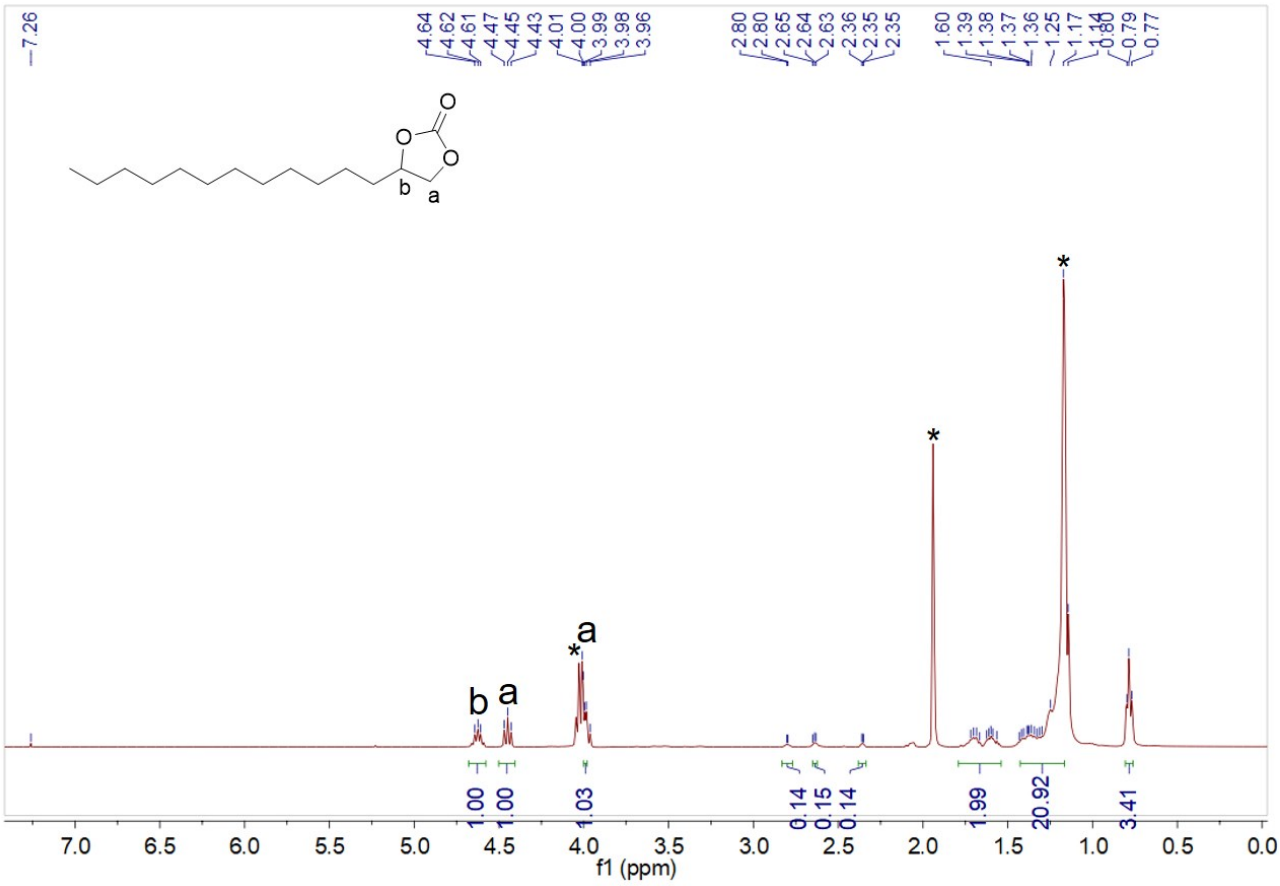

Fig. S18 ^{1}H NMR spectrum of 4-dodecyl-1,3-dioxolan-2-one (400 MHz, $CDCl_3$): δ 4.68~4.58 (1H ,CH_2), 4.45 (1H, CH_2), 3.99 (1H, CH_2), 1.79-1.54 (2H, CH_2), 1.43~1.17 (20H, CH_2), 0.78 ppm (3H, CH_3). * represents the residual solvent ethyl acetate.

References

(S1) Y. Xie, T.-T. Wang, R.-X. Yang, N.-Y. Huang, K. Zou and W.-Q. Deng, *ChemSusChem*, 2014, **7**, 2110-2114.

(S2) Y. Xie, R.-X. Yang, N.-Y. Huang, H.-J. Luo and W.-Q. Deng, *J. Energy Chem*., 2014, **23**, 22-28.

(S3) J. Chen, H. Li, M. Zhong and Q. Yang, *Green Chem*., 2016, **18**, 6493-6500

(S4) Z. Dai, Q. Sun, X. Liu, L. Guo, J. Li, S. Pan, C. Bian, X. Hu, X. Meng, L. Zhao, F. Deng and F.-S. Xiao, *ChemSusChem*, 2017, **10**, 1186-1192.

(S5) Z. Dai, Q. Sun, X. Liu, C. Bian, Q. Wu, S. Pan, L. Wang, X. Meng, F. Deng and F.-S. Xiao, *J. Catal*., 2016, **338**, 202-209.

(S6) S. Wang, K. Song, C. Zhang, Y. Shu, T. Li and B. Tan, *J. Mater. Chem. A*, 2017, **5**, 1509-1515.

(S7) H. Li, C. Li, J. Chen, L. Liu and Q. Yang, *Chem. Asian J*., 2017, **12**, 1095-1103.

(S8) Y. Leng, D. Lu, C. Zhang, P. Jiang, W. Zhang and J. Wang, *Chem. Eur. J*., 2016, **22**, 8368-8375.

(S9) C. Zhang, D. Lu, Y. Leng and P. Jiang, *Mol. Catal*, 2017, **439**, 193-199.

(S10) R. Luo, Y. Chen, Q. He, X. Lin, Q. Xu, X. He, W. Zhang, X. Zhou and H. Ji, *ChemSusChem*, 2017, **10**, 1526-1533.

(S11) Y. Chen, R. Luo, Q. Xu, J. Jiang, X. Zhou and H. Ji, *ChemSusChem*, 2017, **10**, 2534-2541.

(S12) Y. Chen, R. Luo, Q. Xu, J. Jiang, X. Zhou and H. Ji, *ACS Sustainable Chem. Eng*., 2018, **6**, 1074-1082.

(S13) T.-T. Liu, J. Liang, Y.-B. Huang and R. Cao, *Chem. Commun*., 2016, **52**, 13288-13291.

(S14) S. Jayakumar, H. Li, J. Chen and Q. Yang, *ACS Appl. Mater. Interfaces*, 2018, **10**, 2546-2555.

(S15) D. Ma, J. Li, K. Liu, B. Li, C. Li and Z. Shi, *Green Chem*., 2018, **20**, 5285-5291.

(S16) P. Puthiaraj, S. Ravi, K. Yu and W.-S. *Ahn, Appl. Catal*., *B*, 2019, **251**, 195–205.

(S17) W. Wang, C. Li, L. Yan, Y. Wang, M. Jiang and Y. Ding, *ACS Catal*., 2016, **6**, 6091-6100.

(S18) J. Liu, G. Zhao, O. Cheung, L. Jia, Z. Sun and S. Zhang, *Chem. Eur. J*., 2019, **25**, 9052-9059.

(S19) Y. Zhang, N. Luo, J. Xu, K. Liu, S. Zhang, Q. Xu, R. Huang, Z. Long, M. Tong and G. Chen, *Dalton Trans*., 2020, **49**, 11300-11309.